Experimental Verifications and Desing Procedure of an AC-DC Converter with Input Impedance Matching for Wireless Power Transfer Systems

Keisuke Kusaka and Jun-ichi Itoh
Department of Electrical Engineering
Nagaoka University of Technology
Nagaoka, Niigata, Japan
kusaka@stn.nagaokaut.ac.jp, itoh@vos.nagaokaut.ac.jp

***Abstract*—An AC-DC converter with an input impedance matching for the receiving side of wireless power transfer (WPT) systems is mentioned in this paper. WPT systems are desired to operate in high frequency such as 13.56 MHz. In the high-frequency region, input impedance of the AC-DC converter on the receiving side of the WPT systems should be matched to the characteristic impedance of a transmission line because reflected power decreases the transmission efficiency of WPT systems. In this paper, the AC-DC converter with input impedance matching is experimentally demonstrated. Additionally, the design method of the proposed converter is described. First, the validity of the design procedure with using nondimensional parameters is confirmed with a simulation. Then, it is experimentally confirmed that the input impedance of the proposed converter is matched to the 50 + *j*0 Ω at a reflection coefficient of 2.6%. It means that, the reflection coefficient is significantly reduced by 94.5% compared with the conventional diode bridge rectifier (DBR) with a resistive load of 25 Ω.**

I. INTRODUCTION

In recent years, WPT systems with magnetic resonance coupling (MRC) which was reported by A. Karalis et al. in 2007 [1] have been studying increasingly [2-4]. MRC will achieve a high-efficiency transmission at a middle-range transmission distance such as a several dozen of centimeters. In Ref. [5], the 95% transmission efficiency at a transmission distance of 30 cm has been reported. Thus, MRC is a suitable method for applying to a wireless charging system of the battery on an electrical vehicle (EV).

In WPT systems with MRC, the volume and weight of transmission coils strongly depends on the transmission frequency because MRC transmits power with using resonance between the transmission coils. Thus, MRC is expected to operate in a high frequency in order to achieve high power density of the transmission coils. Additionally, MRC should be operated in the industry science medical (ISM) band such as 13.56 MHz. Thereby, the AC-DC converter, which can convert power from 13.56-MHz AC to DC, is necessary in the receiving side of WPT systems. Moreover, the input impedance of the AC-DC converter has to be matched to the characteristic impedance of the transmission line because reflected power, which is caused by the input impedance mismatching in high frequency region, degrades the transmission efficiency of WPT systems with MRC. In Ref. [6], conventional DBR is tested as an AC-DC converter in the receiving side. The Ref [6] pointed out that input impedance matching cannot be achieved because because input impedance of the DBR depends on load conditions. However, the previous studies have not considered the input impedance matching of the AC-DC converter [7].

In this paper, the AC-DC converter, which fulfills the input impedance matching, has been proposed. The proposed AC-DC converter is constructed by the resonant-type rectifier as an input power factor correction (PFC) circuit and the bidirectional boost chopper for stabilizing the operating point of the resonant-type rectifier. It enables a conversion from 13.56-MHz AC to DC without a high-speed dynamic response and a high frequency switching except the diodes. However, the resonant parameters, which determined the input impedance of the proposed converter have decided by a cut and try with a simulation [8]. In this paper, the design procedure of these resonant parameters without a simulation is especially proposed. The intended input impedance is obtained by using nondimensional parameters, which is provided as a specific characteristic of the circuit topology. The validity of the design method is confirmed by the simulation. Then, the input impedance matching characteristics of the proposed AC-DC converter are experimentally evaluated.

II. INPUT IMPEDANCE MATCHING OF AC-DC CONVERTER

A. Requirements for Input Impedance Matching

In this subsection, the requirements for an input impedance matching of an AC-DC converter are described. Generally, high frequency circuits are used with impedance matching in order to suppress reflected power [9]. The impedance matching can be described as; the output impedance of the power supply and the input impedance of the load have equal impedances to the characteristic impedance of the transmission line. In particular, the characteristic impedance of a 50 Ω is used widely. For this reason, 50 Ω is used as the characteristic impedance and the input impedance of the AC-DC converter in this paper.

In general, the characteristic impedance of transmission lines, which is the reference value of the input impedance of the AC-DC converter, does not include an imaginary part. Thus, an input voltage and current of the AC-DC converter are required to fulfill the following requirements, where $\dot{Z}_{in}$ is the input impedance, $\dot{V}_{in}$ is the fundamental input voltage of the AC-DC converter, $\dot{I}_{in}$ is the fundamental input current and θ is the phase angle between the input voltage and the input current.

(a) $\left|\dot{Z}_{in}\right| = \left|\dot{V}_{in}\right| \Big/ \left|\dot{I}_{in}\right| = 50\ \Omega$

(b) Input power factor is 1 ($\cos\theta = 1$)

PFC circuits with a PWM control are used widely in a low frequency region [10]. The PFC circuits with a PWM can satisfy the above-mentioned requirements owing to the input current control. However, a switching frequency for the PWM requires higher frequency than an input frequency. Thus, it is difficult to operate the conventional PFC circuits when the input frequency is constrained in a high frequency such as 13.56 MHz.

Accordingly, an AC-DC converter with a simple circuit configuration, which can achieve the input impedance matching, is required in the receiving side of WPT systems.

B. Proposed AC-DC Converter with Input Impedance Matching

Fig. 1 presents the circuit configuration of the proposed AC-DC converter. The proposed converter consists of the improved resonant-type rectifier and the bidirectional boost chopper. The resonant-type rectifier is originally proposed by K. Matsui et al. [11].

Ref. [11] has evaluated the resonant-type rectifier merely from a standpoint of the rectifier with a PFC in a commercial frequency. In contrast, this paper aims to make the input impedance matching of the AC-DC converter with using the resonant-type rectifier in the frequency of 13.56 MHz.

The low frequency operation causes a low power density because the resonant-type rectifier works with using resonance between the resonance inductor L_1, which is connected in series to the input terminal and resonance

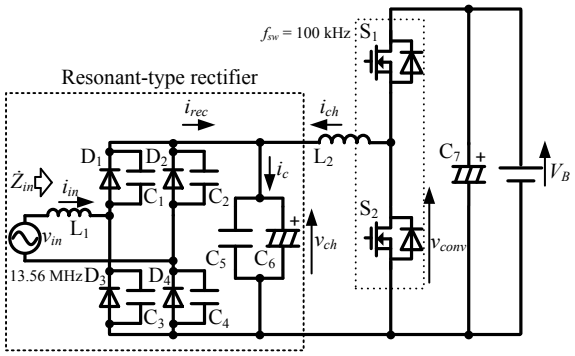

Figure 1. Proposed AC-DC converter with input impedance matching.

capacitors $C_{1\text{-}4}$. In Ref. [10], the resonant-type rectifier is operated in a commercial frequency. In a commercial frequency, bulk resonance components are needed. Thus, the resonant-type rectifier is not effective from a standpoint of the PFC converter in the commercial frequency. Meanwhile, the resonant-type rectifier is used in a high frequency such as a 13.56 MHz in this paper. It will improve the power density of the converter.

Note that, the original resonant-type rectifier has only two resonance capacitors $C_{1\text{-}2}$ connected in parallel to the diodes on an upper arm [12]. By contrast, the additional capacitors $C_{3\text{-}4}$ are added into the lower arm in order to improve the high frequency characteristics in this paper.

Additionally, it has pointed that the amplitude of the input current and the input power factor are changed by load conditions when a resistive load is connected directly to the resonant-type rectifier [12]. In other words, the input impedance of the stand-alone resonant-type rectifier is fluctuated depending on the load conditions. For the input impedance matching, the input power factor should be unity constantly regardless of the load conditions. In order to solve this problem, the bidirectional boost chopper is connected at the output side of the improved resonant-type rectifier as shown in Fig. 1. The bidirectional boost chopper is used to adjust the operating point of the resonant-type rectifier through an automatic voltage regulator in term of the rectifier output voltage; v_{ch}. Thus, the proposed AC-DC converter enables a conversion from 13.56-MHz AC to DC without a high frequency switching except the diodes. Note that, the silicon carbide (SiC) schottky barrier diodes (SiC-SBDs) are used as a rectifying device in order to rectify the high frequency input.

C. Control Method of the Proposed Converter

The input impedance of the proposed converter is determined by the resonance parameters; the resonance inductance $L = L_1$, the resonance capacitances $C = C_1 = C_2 = C_3 = C_4$ and the voltage ratio α_V. The intended input impedance can be obtained by designing these parameters according to the design procedure, which is described in chapter IV. Note that the voltage ratio is the ratio of the rectifier output voltage v_{ch} to the maximum input voltage V_m.

In the proposed circuit, the voltage ratio should be controlled by the bidirectional boost chopper in order to stabilize the input impedance because the voltage ratio depends on the input power. Note that, the input power can be controlled by only an input voltage when an input impedance is constant. Thus, the rectifier output voltage is controlled by the bidirectional boost chopper with PI control.

Fig. 2 shows the control block diagram of the proposed converter. The proposed circuit controls the rectifier output voltage v_{ch} through the control of the inductor current i_{ch}. The controller is constructed by the automatic voltage regulator (AVR) and the automatic current regulator (ACR) which is included in the AVR as an inner loop. The natural angular frequencies of the AVR and ACR are designed as 400 rad/s and 4000 rad/s respectively. In Fig. 2, T_{ic} is the integral time of the ACR and T_{iv} is the integral time of the AVR. The proposed converter does not need a high-speed dynamic response when the capacitance C_4 is sufficiently large to neglect the voltage ripple. It means that proposed circuit does not need a high-speed dynamic response and high frequency switching.

The reference voltage value of the bidirectional boost chopper v_{ch}^* is calculated from (1) with using a reference value of the voltage ratio α_V^* because the voltage ratio has to be maintained constant.

$$v_{ch}^* = V_m \times \alpha_V^* \tag{1}$$

III. Operation Modes of the Proposed Circuit

In this chapter, the operation modes of the proposed AC-DC converter are described. Especially, the input current is mathematically analyzed.

Fig. 3 shows the each operation mode of the proposed converter. Note that, the bidirectional boost chopper is drawn as an ideal voltage source in a schematics because the bidirectional boost chopper with the voltage control and large capacitance C_4 can be assumed as an ideal voltage source.

Fig. 4 presents the simplified waveforms of the proposed circuit with a unity input power factor. The each circuit operation is explained in the following statements. In this consideration, forward voltage drops of the diodes are ignored for simplicity.

A. Operation Mode I

In this mode, the input current starts to flow with an increase of the input voltage. The input current flows through the paths; L_1-C_1-C_2 and L_1-C_3-C_4. Note that, the initial current on the resonance inductor at the start of this mode is assumed as zero. Additionally the resonance capacitors C_1 and C_4 have charged while the mode III in the previous period. Thus, the capacitor voltage prevents the diodes D_1 and D_4 from turning on. From a circuit equation, input current i_{in_I} is derived as (2).

$$i_{in\_I}(t) = \frac{\omega_{in}\omega_1^2 C V_m}{\left(\omega_{in}^2 - \omega_1^2\right)}\left(\cos\omega_1 t - \cos\omega_{in} t\right) + \omega_1 C v_{ch}\sin\omega_1 t \tag{2}$$

where V_m is the maximum input voltage, ω_{in} is the input angular frequency and ω_1 is the resonance frequency which is expressed by (3). The resonance angular frequency is defined as resonance between the combined capacitors and the resonance inductor.

$$\omega_1 = \frac{1}{\sqrt{LC}} \tag{3}$$

From (2), the input current has two frequency components; the resonance angular frequency ω_1 and the input angular frequency ω_{in}. Thus, the input current has distortion.

The input current gradually discharge and charge the resonance capacitors C_1, C_4 and C_2, C_3 respectively while this mode. After the capacitor voltage v_{cv} reaches to the DC voltage v_{ch}, the next operation mode starts.

Incidentally, the period of the operation mode I; T_I is equal to the discharging time of the capacitor C_1. Thus, the period T_I can be derived from (4) with the numerical analytical approach.

$$\frac{v_{ch}}{2}\left(1+\cos\omega_1 T_1\right) + \frac{\omega_1 V_m}{2\left(\omega_{in}^2 - \omega_1^2\right)}\left(\omega_1\sin\omega_{in}T_1 - \omega_{in}\sin\omega_1 T_1\right) = 0 \tag{4}$$

B. Operation Mode II

The input current commutates to the diodes D_1 from the

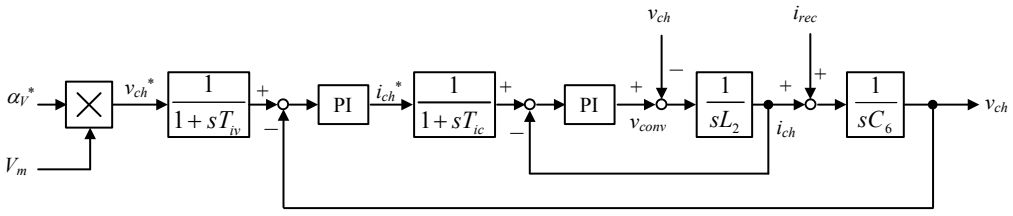

Figure 2. Control block diagram for the proposed circuit.

capacitor C_1 because the diodes D_1 and D_4 become a turn-on. The input current flows into the path that is formed by inductor L_1, diodes D_1 and D_4. In this mode, the smoothing capacitor is charged by the input current, which is expressed by (5), where $i_{in\_I}(T_1) = i_{in\_II}(T_1)$ and ω_2 is the resonance angular frequency expressed by (6). The input current in the mode II is not a complete sinusoidal waveform also.

$$i_{in\_II}(t) = i_{in\_I}(T_1)\cos\omega_2(t-T_I) - \frac{v_{ch}}{\omega_2 L}\sin\omega_2(t-T_I) + \frac{V_m\cos\omega_{in}T_I}{(\omega_{in}^2-\omega_2^2)L}\{\omega_{in}\cos\omega_2(t-T_I) - \omega_{in}\cos\omega_{in}(t-T_I)\} + \frac{V_m\sin\omega_{in}T_I}{(\omega_{in}^2-\omega_2^2)L}\{\omega_{in}\sin\omega_{in}(t-T_I) - \omega_2\sin\omega_2(t-T_I)\} \quad (5)$$

$$\omega_2 = \frac{1}{\sqrt{L(C_5+C_6)}} \quad (6)$$

Incidentally, (5) can be simplified to (7) when the resonance angular frequency ω_2 is sufficiently small to be ignored. In the proposed circuit topology, the capacitance C_6 is sufficiently large in general for the purpose to stabilize the operation of the bidirectional boost chopper.

$$i_{in\_II}(t) \approx i_{in\_I}(T_1) - \frac{v_{ch}}{L}(t-T_1) + \frac{V_m}{\omega_{in}L}(\cos\omega_{in}T_1 - \cos\omega_{in}t) \quad (7)$$

Besides, the capacitor voltages v_{cu} and v_{cv} are not changed in this mode. The mode II continues until the input voltage polarity is changed from the positive to the negative.

C. Operation Mode III

In this mode, the input current flows in the opposite direction to the mode I via C_2-C_1-L_1 and C_4-C_3-L_1. In this mode, the input current is expressed by $i_{in\_III}(t) = - i_{in\_I}(t\text{-}T/2)$ where T is the period of the AC input. The capacitors C_2 and C_1 are discharged and charged respectively by the input current. The mode III continues until the capacitor voltage v_{cu} reaches to the DC voltage v_{ch}. The period of the mode III is same to the period of the mode I.

D. Operation Mode IV

The input current commutates to the diodes D_2 and D_3 from the capacitors C_1 and C_2. The input current is expressed by $i_{in\_IV}(t) = -i_{in\_II}(t\text{-}T/2)$.

According to the input current equations (2) and (7), the amplitude of the input current and the input power factor are determined by the resonance parameters; capacitances C_1, C_2 and inductance L_1, and the relation between the maximum input voltage V_m and rectifier output voltage v_{ch}. Hence the intended input impedance of the AC-DC converter can be

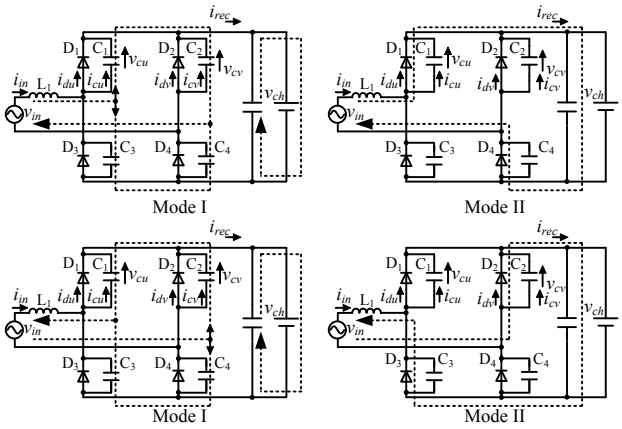

Figure 3. Operation modes of the proposed AC-DC converter with input impedance matching.

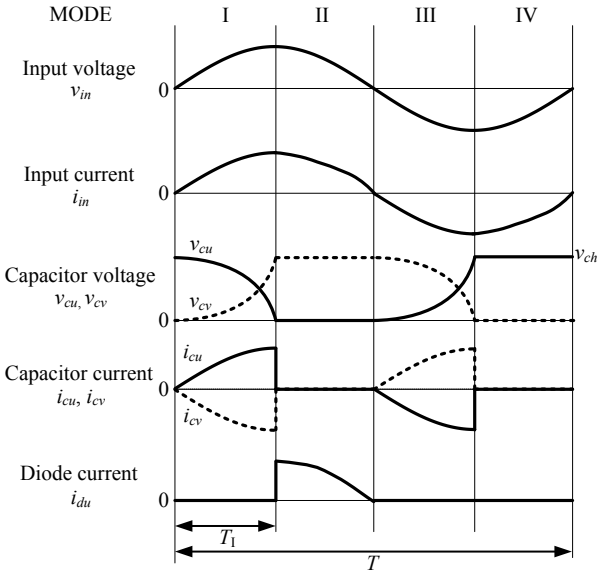

Figure 4. Simplified waveforms of the proposed circuit.

obtained by designing these parameters properly. The design method is explained in the following chapter.

IV. Design Procedure

Fig. 5 shows the design flowchart of the circuit parameters. In order to obtain the intended input impedance of the proposed converter, the relationship among the resonance parameters and rectifier output voltage should be designed properly. Table I presents the parameters, which are used in the design procedure.

The real part of the input impedance $\mathrm{Re}[\dot{Z}_{in}]$, the rated input power P_{in}, the minimum battery voltage V_B and input frequency f_{in} are fed in compliance with the procedure as a specification. Note that, the real part of the input impedance is equal to the absolute value of the input impedance because the characteristic impedance of the co does not include an

imaginary part in general. In other words, the imaginary part of the required input impedance is zero.

1) Step 1: Derivation of Maximum Input Voltage V_m

When the input power factor is unity, the maximum input voltage of the sinusoidal wave for obtaining the required rated input power P_{in} is expressed by

$$V_m = \sqrt{2P_{in}\,\mathrm{Re}[\dot{Z}_{in}]} \qquad (8).$$

2) Step 2: Decision of Rectifier Output Voltage v_{ch}

The rectifier output voltage is decided with fulfilling $V_m<v_{ch}<V_B$. The resonant-type rectifier and the bidirectional boost chopper impose this restriction because the resonant-type rectifier works with a boost of voltage. Moreover, the bidirectional boost chopper is used at the output side of the resonant-type rectifier for purpose of maintaining the voltage. Thus, this restriction will be changed where other circuit topologies are used.

3) Step 3: Calculation of Voltage Ratio α_V

The voltage ratio α_V is defined in (9). The rectifier output voltage is controlled to maintain the voltage ratio at a constant even when the input power is changed. The voltage ratio, which is designed in here, is provided to Fig. 2 as a reference value.

$$a_V = v_{ch}/V_m \qquad (9)$$

4) Step 4: Derivation of Frequency Ratio α_f

The frequency ratio is defined as (10) where f_{re} is the resonance frequency, which is expressed by (11), and f_{in} is the input frequency.

$$\alpha_f = f_{re}/f_{in} \qquad (10)$$

$$f_{re} = \frac{1}{2\pi\sqrt{LC/2}} \qquad (11)$$

Fig. 6 shows the relationship between the voltage ratio and the frequency ratio, which achieves unity input power factor. The unity input power factor is achieved by the proper choice of the frequency ratio from the approximate expression. Equation (12) expresses the approximated curve.

$$\alpha_f \approx -1.680a_V^3 + 9.045\alpha_V^2 - 16.616\alpha_V + 12.248 \qquad (12)$$

This approximated curve is derived from numerical analysis based on circuit simulation because the relationship between the frequency ratio and the voltage ratio is a non-linearly characteristic. However, both the frequency ratio and voltage ratio are nondimensional parameters. For this reason, the specified relationship between the frequency ratio α_f and the voltage ratio α_V is provided regardless of any other parameters.

TABLE I. PARAMETERS USED IN DESIGN PROCEDURE.

Parameters	Symbol	Unit	Definition
Input impedance	$\dot{Z}_{in}$	Ω	
Input power	P_{in}	W	
Input maximum voltage	V_m	V	
Rectifier output voltage	v_{ch}	V	
Battery voltage	V_B	V	Minimum value
Input frequency	f_{in}	Hz	
Resonance frequency	f_{re}	Hz	$f_{re}=\frac{1}{2\pi\sqrt{LC/2}}$
Resonance inductance	L	H	
Resonance capacitance	C	F	
Frequency ratio	α_f	Non dimensional	$\alpha_f = f_{re}/f_{in}$
Voltage ratio	α_V	Non dimensional	$a_V = v_{ch}/V_m$
Parameter for determining absolute vlaue of input impedance	β	Non dimensional	$\beta=\frac{\mathrm{Re}[\dot{Z}_{in}]}{\omega_{in}L}$

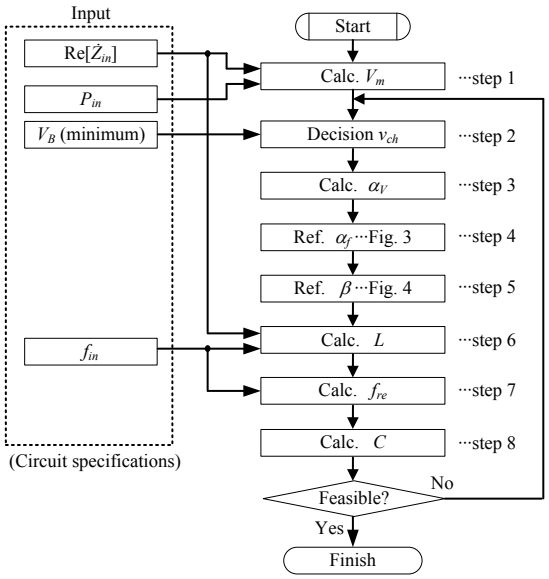

Figure 5. Flowchart of the circuit design.

5) Step 5: Derivation of Nondimensional Parameter β

Fig. 7 shows the relationship between the voltage ratio and the nondimensional parameter β where the input power factor is inevitably one owing to step 4. This curve is also derived from numerical analysis based on circuit simulation. The parameter β for obtaining the intended absolute value of the input impedance can be read from the approximated curve. Both the voltage ratio and parameter β are nondimensional. Thus, the simulated curve is provided regardless of any other parameters. The approximation formula is expressed by

$$\beta \approx -0.642a_V^3 + 3.630\alpha_V^2 - 7.132\alpha_V + 5.348 \qquad (13).$$

The parameter β is defined as (14). It is a ratio of the resonance inductance L to the absolute value of the input impedance Re[$\dot{Z}_{in}$] with a normalization by the input angular frequency ω_{in} (= $2\pi f_{in}$).

$$\beta = \frac{\mathrm{Re}[\dot{Z}_{in}]}{\omega_{in} L} \tag{14}$$

6) Step 6: Calculation of Resonance Inductance L

The resonance inductance, which is needed to obtain the intended input impedance Re[$\dot{Z}_{in}$], is calculated from (14).

7) Step 7: Calculation of Resonance Frequency

The resonance frequency is calculated by the definition of frequency ratio α_f shown as (10) using the input frequency f_{in}.

8) Step 8: Calculation of Resonance Capacitance C

The resonance capacitance is calculated by (15).

$$C = \frac{1}{2\pi^2 f_{re}^2 L} \tag{15}$$

V. Simulation Results

Fig. 8 provides the simulation waveforms of the proposed AC-DC converter. The simulation parameters are shown in Table II, which were designed according to the design procedure. The simulation results performs that the control of the bidirectional boost chopper is correctly operated. Namely, the rectifier output voltage v_{ch} and chopper current i_{ch} track to the each reference value.

Moreover, a sinusoidal input current and unity input power factor are achieved. In this simulation, the input impedance is calculated from the fundamental component of the input voltage and input current as 50.1 + j0.9 Ω with using (16), where V_{in_1st} is the fundamental component of the input voltage, I_{in_1st} is the fundamental component of the input current and θ is the phase angle between the input voltage and input current of the fundamental component.

From the simulation results, it is confirmed that the input impedance can be designed correctly by the design procedure.

$$\dot{Z}_{in} = \frac{|V_{in\_1st}|}{|I_{in\_1st}|}\cos\theta + j\frac{|V_{in\_1st}|}{|I_{in\_1st}|}\sin\theta \tag{16}$$

It means that the proposed converter is capable of the input impedance matching to the 50 + j0 Ω at a reflection coefficient of 0.87%. The reflection coefficient is defined by (17) where $\dot{Z}_0$ is the characteristic impedance, P_F is the supplied travelling power to the AC-DC converter, P_R is the reflected power, which occurs at the input terminal of the AC-DC converter. The reflection coefficient is used widely in a research field of high-frequency circuits in order to evaluate the circuit performance.

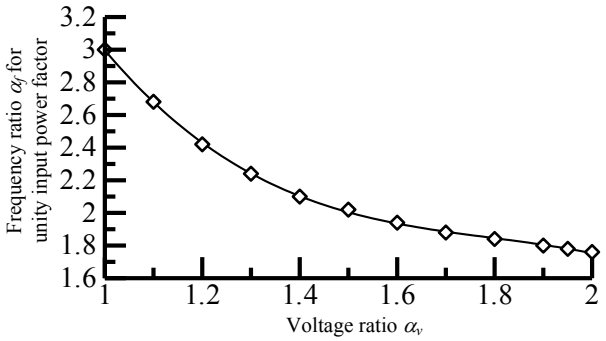

Figure 6. Requirement of unity input power factor.

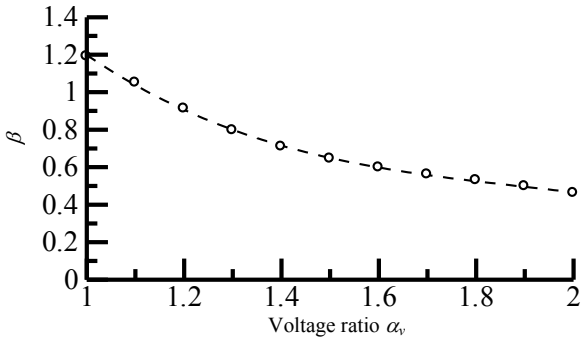

Figure 7. Parameter β for designing an absolute value of the input impedance.

TABLE II. Simulation Parameters.

Specifications			
Parameters	Symbol	Value	Unit
Input impedance	$\dot{Z}_{in}$	50+j0	Ω
Input power	P_{in}	500	W
Battery voltage	V_B	300	V
Input frequency	f_{in}	13.56	MHz
Designed value			
Rectifier output voltage	v_{ch}	240	V
Resonance inductance	L	578	nH
Resonance capacitance	C	68.9	pF
Frequency ratio	α_f	2.63	Non dimensional
Voltage ratio	α_V	1.12	Non dimensional
Parameter for determining absolute vlaue of input impedance	β	1.01	Non dimensional

$$\Gamma = \left|\frac{\dot{Z}_0 - \dot{Z}_{in}}{\dot{Z}_0 + \dot{Z}_{in}}\right| = \sqrt{\frac{P_R}{P_F}} \tag{17}$$

The reflection coefficient does not reach to zero due to the error on the approximated curve. However, the effects of the error are small to be ignored.

VI. EXPERIMENTAL RESULTS

A. Fundamental Characteirstics

Table III provides the parameters of the experimental setup. In this paper, only the parasitic capacitances of the diodes are used as a resonance capacitor. The parasitic capacitances value is estimated from the datasheet of the products. Note that the proposed converter is constructed on the PCB for purpose of reducing parasitic inductances of wires.

Fig. 9 presents the experimental waveforms of the proposed AC-DC converter. It is clear that a power conversion from 13.56 MHz to DC is achieved by the proposed converter. Additionally, the sinusoidal input current and unity input power factor is obtained. It means that the design method is valid for obtaining the intended input impedance.

Fig. 10 shows the harmonics analysis results of the input voltage and current, which is conducted in order to derive the input impedance from the experimental waveforms shown in Fig. 9. Note that, the probes; a differential probe (Tektronix, P5205) and a current probe (Tektronix, TCP312) which are used in these experiments, provide a limitation to the frequency bandwidth at 100 MHz. For this reason, the harmonics components over seventh should be considered as reference values. From the fundamental components of the input voltage and input current, the input impedance of the proposed converter is calculated as $\dot{Z}_{in}$ = 52.7 - j0.02 Ω. The measured reflection coefficient is Γ = 2.6%. The input current total harmonic distortion (THD) of 8.1% (reference value) is performed with the bandwidth up to 20th.

B. Comparison of the Reflection Coefficient

In this subsection, the reflection coefficients are compared between the conventional DBR and the proposed converter.

Generally, the input impedance matching of the DBR is never achieved in the reason of the distorted input current and low input power factor. Moreover, the reflection coefficient of the conventional DBR depends on the load conditions and a smoothing capacitor widely. In contrast, the reflection coefficient of the proposed circuit does not depend on the load condition and a value of the smoothing capacitor.

Fig. 11 shows the comparison result of the reflection coefficient. Note that, the conventional DBR has a smoothing capacitor of 0.47 μF. The proposed converter achieves the input impedance matching with the reflection coefficients of 2.6%. It is clear that the reflection coefficient can be suppressed compared to the conventional DBR. In particular, the reflection coefficient with the improved AC-DC converter suppresses the reflection coefficient by 94.5 % compared with the conventional DBR with a load of 25 Ω.

VII. CONCLUSION

In this paper, the input impedance matching of the AC-DC converter for the receiving side of WPT systems is

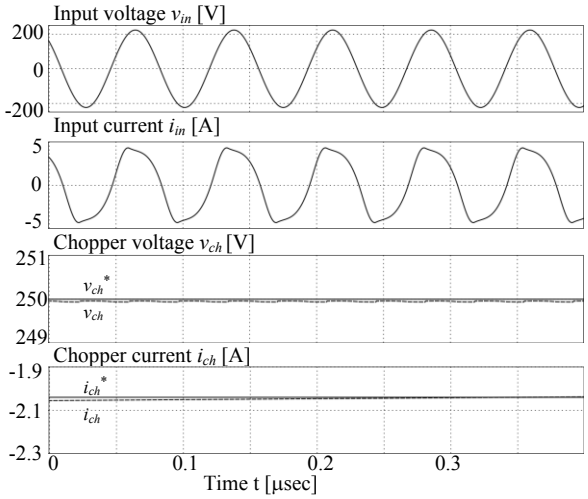

Figure 8. Simulation result of the proposed AC-DC converter.

TABLE III. PARAMETERS OF THE EXPERIMENTAL SETUP.

Items		Manufactures	Model number	Value
MOSFET	S_1, S_2	Vishay	IRFB11N50APBF	500 V, 11 A
Diode	D_1-D_4	Cree	C3D08060A	600 V, 8 A
Inductor	L_1	TDK	VLF10040T-1R5N8R9	1.5 μH
	L_2	-	-	2.3 mH
Capacitor	C_{1-4}	-	(Parasitic capacitances of the diodes)	(34.3 pF)
	C_5	TDK	CKG57NX7R2J474M	470 nF (in parallel)
	C_6	Nichicon	UPW2V221MRD	220 μF (in parallel)
	C_7	BHC Components	ALS30A221DB450	220 μF

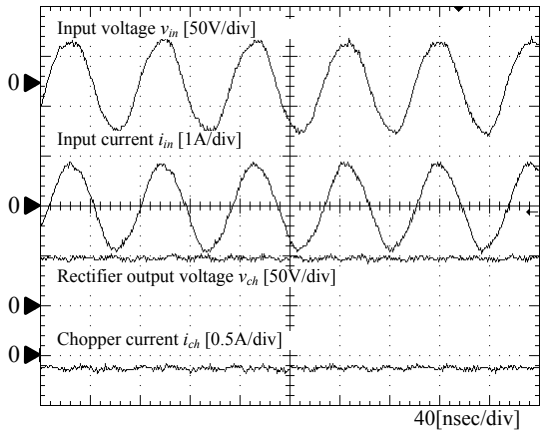

Figure 9. Experimental waveforms of the proposed AC-DC converter.

mentioned. In the high frequency such as a 13.56 MHz reflected power decrease the transmission efficiency of the WPT systems. In order to overcome this problem, the AC-DC converter, which achieves the input impedance, was proposed. The AC-DC converter achieves the input impedance matching using resonance. In this paper, the design method of these resonance parameters is presented and confirmed by the simulation.

Additionally, the AC-DC converter is experimentally tested. From the experimental results, the input impedance of the converter is obtained as $\dot{Z}_{in}$ = 52.7 - *j*0.02 Ω. The proposed AC-DC converter performed the reflection coefficient of 2.6%. From the comparison results on the reflection coefficient between the proposed AC-DC converter and the DBR, the proposed converter suppresses the reflection coefficient. In particular, the reflection coefficient is suppresses by 94.5% compared with the conventional DBR with a resistive load of 25 Ω.

ACKNOWLEDGMENT

This work was supported by Japan Society for the Promotion of Science; Grant-in-Aid for Scientific Research (B), 2436016.

REFERENCES

[1] A. Kurs, A. Karalis, R. Moffatt, J. D. Joannopoulos, P. Fisher, M. Soljacic: "Wireless Power Transfer via Strongly Coupled Magnetic Resonances", Science, Vol. 317, pp. 83-86 (2007)

[2] J. J. Casanova, Z. N. Low, J. Lin: "A Loosely Coupled Planar Wireless Power System for Multiple Receivers", IEEE Trans. On Industrial Electronics, Vol. 56, No. 8, pp. 3060-3068 (2009)

[3] S. Cheon, Y. Kim, S. Kang, M. L. Lee, J. Lee, T. Zyung: "Circuit-Model-Based Analysis of a Wireless Energy-Transfer System via Coupled Magnetic Resonances", IEEE Trans. On Industrial Electronics, Vol. 58, No. 7, pp. 2906-2914 (2011)

[4] T. Imura, Y. Hori: "Maximizing Air Gap and Efficiency of Magnetic Resonant Coupling for Wireless Power Transfer Using Equivalent Circuit and Neumann Formula", IEEE Trans. On Industrial Electronics, Vol. 58, No. 10, pp. 4746-4752 (2011)

[5] S. Lee, R. D. Lorenz: "Development and Validation of Model for 95%-Efficiency 200-W Wireless Power Transfer Over a 30-cm Air-gap", *IEEE Trans. On Industry Applications*, Vol. 47, No. 6, pp. 2495-2504 (2011)

[6] K. Kusaka, J. Itoh, "Experimental Verification of Rectifiers with SiC/GaN for Wireless Power Transfer Using a Magnetic Resonance Coupling," The 9th IEEE International Conference on Power Electronics and Drive Systems, No. 380, pp. 1094-1099 (2011)

[7] T. C. Beh, M. Kato, T. Imura, S. Oh, Y. Hori: "Automated Impedance Matching System for Robust Wireless Power Transfer via Magnetic Resonance Coupling", IEEE Trans. On Industrial Electronics, Vol. PP, No. 99, pp. 1-10 (2011)

[8] K. Kusaka, J. Itoh, "Input Impedance Matched AC-DC Converter in Wireless Power Transfer for EV Charger", The 15th International Conference on Electrical Machines and Systems 2012, LS2A-2 (2012)

[9] J. R. Long: "Monolithic Transformers for Silicon RF IC Design", IEEE Trans. On Solid-state Circuits, Vol. 35, No. 9, pp. 1368-1382 (2000)

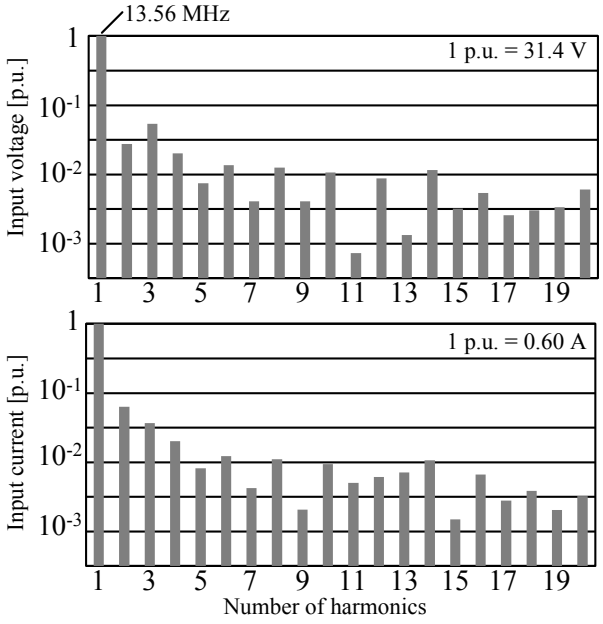

Figure 10. Harmonics analysis of the input voltage and input current of the proposed AC-DC converter.

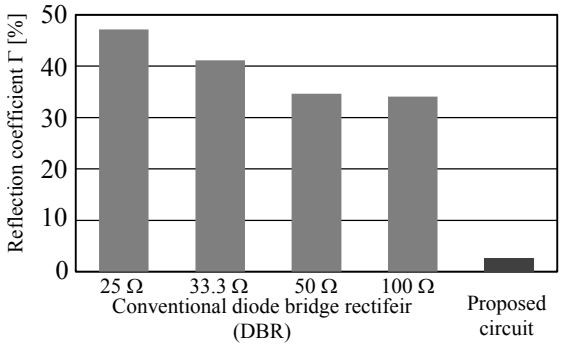

Figure 11. Comparison of the reflection coefficient between the conventional CI-DBR and proposed circuit.

[10] B. Singh, B. N. Singh, A. Chandra, K. Al-Haddad, A. Pandey, D. P. Kothari: "A Review of Single-Phase Improved Power Quality AC-DC Converters", IEEE Trans. On Industrial Electronics, Vol. 50, No. 5, pp. 962-981 (2003)

[11] K. Matsui, I. Yamamoto, G. Erdong, M. Hasegawa, K. Ando, F. Ueda, H. Mori, "A High DC voltage Generator by LC Resonance in Commercial Frequency", Power Conversion Conference 2007, pp. 1093-1098 (2007)

[12] K. Matsui, I. Yamamoto, K. Ando, G. Erdong: "A Novel High DC Voltage Generator by LC Resonance in Supply Frequency", EPE2007, pp. 1-8 (2007)